

## Formation of intermetallic compounds upon cooling of $\text{Sn}_{1-x}\text{Zr}_x$ melts

S. MUDRY<sup>1</sup>, U.E. KLOTZ<sup>2</sup>, A. KOROLYSHYN<sup>1</sup>, I. SHTABLAVYI<sup>1\*</sup>

<sup>1</sup> Physics of Metals Department, Ivan Franko National University of Lviv, Kyrylo and Mephodii str. 8, 79005 Lviv, Ukraine

<sup>2</sup> EMPA, Dübendorf, Switzerland

\* Corresponding author. Tel.: +380-322-394594. E-mail: sihor@ukr.net

Received October 16, 2007; accepted May 15, 2008; available on-line September 10, 2008

The structure of  $\text{Sn}_{1-x}\text{Zr}_x$  ( $x = 0.02, 0.05, 0.15, 0.25, 0.35, 0.45$ ) alloys has been studied by means of X-ray diffraction methods at different temperatures. The structure factors, pair correlation functions and main parameters have been analyzed. It is shown that the structure of Sn-enriched liquid alloys is inhomogeneous in the region of pre-crystallization temperatures. The solidified phases created upon cooling are in agreement with those present in the equilibrium phase diagram. The X-ray diffraction data were used to determine more exactly the temperatures of the liquidus curve, which is not yet completely investigated.

### Tin-based melts / Brazing / Phase diagrams

#### Introduction

Alloys of tin with zirconium are interesting due to their use as brazing materials [1,2]. The brazing process is based on the tendency to form intermetallic compounds by means of liquid-solid reaction. The kinetics of this reaction and properties of the solidified phases depend significantly on concentration, temperature and cooling rate. Information on these parameters, commonly estimated from phase equilibrium diagrams, is poor, because the Sn-Zr phase diagram in the Sn-rich region, especially the 'liquidus' curve, is not completely established [3]. All these reasons motivated structure studies of  $\text{Sn}_{1-x}\text{Zr}_x$  alloys starting from the liquid state.

The binary Sn-Zr system reveals three intermetallics:  $\text{ZrSn}_2$ ,  $\text{Zr}_5\text{Sn}_3$  and  $\text{ZrSn}_4$  (Fig. 1). The first and last of them are formed according to peritectic reactions, whereas  $\text{Zr}_5\text{Sn}_3$  is formed from the liquid state. Some regions of the liquidus curve, as well as the extension of the homogeneity range of the  $\text{Zr}_5\text{Sn}_3$  compound, are predicted or probable.

#### Experimental

Samples of  $\text{Sn}_{1-x}\text{Zr}_x$  ( $x = 0.02, 0.05, 0.15, 0.25, 0.35, 0.45$ ) were prepared under argon atmosphere in an arc melting furnace and checked by X-ray analysis. The diffraction studies were carried out using a high-temperature diffractometer with a special attachment

that makes it possible to investigate solid and liquid samples at different temperatures up to 2000 K.  $\text{Cu-K}\alpha$  radiation, monochromatized by means of a LiF single crystal, and Bragg-Brentano focusing geometry were used. The scattered intensities as a function of the scattering angle were recorded within the range  $1\text{\AA}^{-1} < k < 7\text{\AA}^{-1}$ , with different angular steps, which were equal to  $0.05^\circ$  within the region of the principal peak and  $0.5^\circ$  for the remaining values of the wave vector.

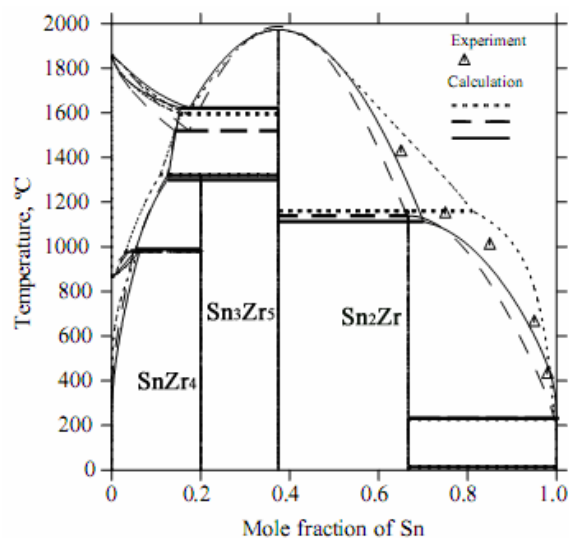


Fig. 1 Comparison between the calculated phase diagram of the Sn-Zr system [3-5] and experimental data [6].

**Table 1** Structural parameters of Sn<sub>1-x</sub>Zr<sub>x</sub> melts.

<i>x</i>	$k_1, \text{\AA}^{-1}$	$k_2, \text{\AA}^{-1}$	$S(k_1)$	$r_1, \text{\AA}$	$r_2, \text{\AA}$	<i>Z</i>	$T_L, \text{K}$
Sn	2.21	4.35	2.28	3.23	6.3	10.9	-
0.02	2.3	4.34	2.39	3.19	5.98	10.3	702
0.05	2.34	4.29	2.34	3.19	6.03	10.5	934
0.15	2.27	4.34	2.25	3.2	6.07	10.1	1280
0.25	2.27	4.33	2.25	3.2	6.07	10.2	1420
Zr	2.32	4.37	2.35	3.19	6.0	10.6	-

$k_1$  – first peak position of structure factor

$k_2$  – second peak position of structure factor

$S(k_1)$  – height of principal peak of structure factor

$r_1, r_2$  – most probable interatomic distances

*Z* – number of neighbors

$T_L$  – “liquidus” temperature

The scattered intensity was measured with accuracy better than 2 %. In order to obtain more accurate scattered intensities, the scan time was equal to 100 s. The diffracted intensity was recorded using a NaI(Tl) scintillation detector in conjunction with an amplification system. The sample was placed in a rounded cup of 20 mm diameter.

Scattered intensities as a function of the scattering angle were recorded and corrected for absorption, anomalous dispersion and incoherent scattering [7].

The structure factors (SF) were obtained from the angular dependence of the scattered intensities. Pair correlation functions (PCF) were calculated from SF by means of Fourier-transformation. From these functions the main structure parameters – first and second peak positions  $k_1$ ,  $k_2$ ,  $r_1$ ,  $r_2$ , number of neighbors *Z*, and height of the first peak  $a(k_1)$  were determined.

## Results and discussion

The structure factor for the liquid Sn<sub>0.98</sub>Zr<sub>0.02</sub> alloy is shown in Fig. 2a and is similar to the one of liquid tin. Nevertheless, a comparison of the main parameters –  $k_1$ ,  $k_2$  – positions of the first and second maxima, as well as  $s(k_1)$  – height of the principal peak, reveal some discrepancies between them (Table 1). Similar features are also observed for the pair correlation functions. In particular, the most probable interatomic distances are significantly reduced in comparison with liquid tin. Taking into account this feature one can suppose that the liquid Sn<sub>0.98</sub>Zr<sub>0.02</sub> alloy cannot be considered as a solution with random atomic distribution. Consequently, although the content of Zr is small, its influence on the structure in the liquid state is considerable.

Upon cooling of the melt, below a certain temperature the diffraction patterns reveal peaks corresponding to crystalline phases. The density of the crystallites is less than that of the liquid phase and for this reason they swim on the surface of the melt. Consequently the temperature at which the crystalline like peaks appear in the background of the diffraction

pattern for the liquid phase, can be considered as a point determining the “liquidus” curve. The peaks corresponding to the crystalline phases are very wide due to the small crystallite size. The identification of the peaks, which show higher resolution at lower temperature (Fig. 2a), allowed us to reveal the coexistence of solid Sn and ZrSn<sub>2</sub>, which is in accordance with the recently published phase diagram [3-5].

An increase of the Zr content to 5 at.% (Fig. 2b) produced no significant changes in the structure factor, in comparison with the melt of the previous concentration. The positions of the principal peak,  $k_1$ , and of the second one,  $k_2$ , change in opposite directions.  $k_1$  increases, whereas the  $k_2$  value is reduced. The most probable interatomic distance  $r_1$  is the same, but the  $r_2$  parameter slightly increases. The number of neighbours *Z* remains practically constant. An analysis of these parameters allowed us to conclude that the Zr-atoms tend to influence the atomic distribution of tin also in the melt of this concentration.

Upon cooling below the liquidus temperature the crystalline phase appears. The analysis of the diffraction patterns recorded at a temperature corresponding to a two-phase mixture and at room temperature revealed the crystallization of ZrSn<sub>2</sub> and tin. These two phases exist also at room temperature, which is in accordance with the equilibrium phase diagram.

With a further increase of the Zr-atom content (15; 25 at.% Zr) the tin-like profile of the structure factor persists, showing almost unchanged parameters. Nevertheless it should be noted here that when the content of Zr is larger than 5 at.% an essential reduction of the structure factor of the principal peak,  $S(k_1)$ , is observed. Such a reduction is attributed to a decrease of the density of the melt, which is supposed to be caused by an increase of structure inhomogeneities. Beside the tin-based matrix, where Zr-atoms are diluted, chemically ordered ZrSn<sub>2</sub>-associates are assumed to be formed in melts with higher Zr content.

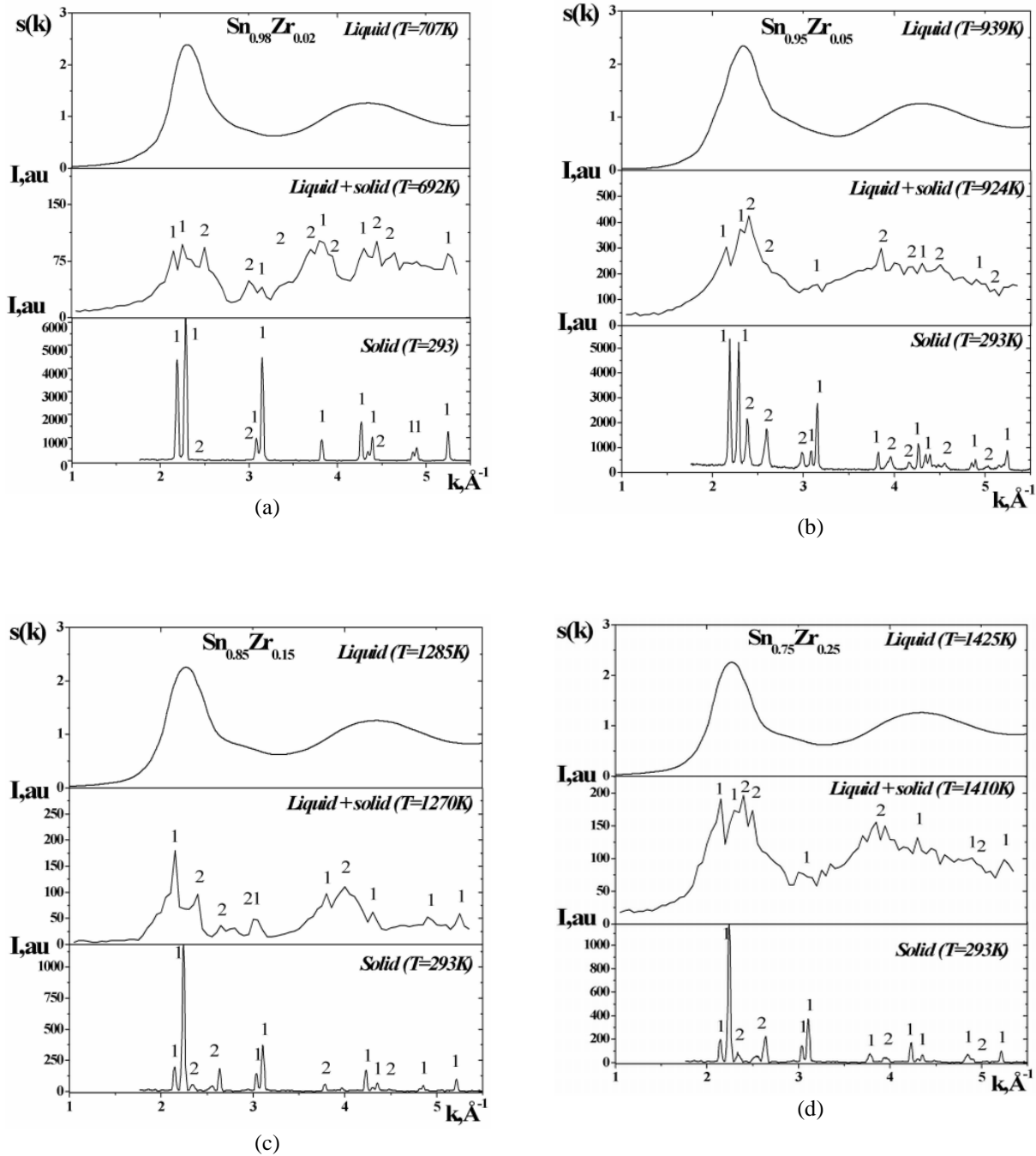


**Fig. 2** Structure changes in  $\text{Sn}_{1-x}\text{Zr}_x$  molten alloys ( $x = 0.02$  (a);  $0.05$  (b);  $0.15$  (c);  $0.25$  (d)), (1-Sn; 2-  $\text{ZrSn}_2$ ).

It can be seen from the table that the number of neighbors  $Z$  is less than the corresponding parameters for liquid Zr and Sn. The reason for such a difference is supposed to be a partial localization of electrons, which produces the formation of some covalency in the bonding between the atoms in the associates. Chemical ordering obtained in such a way decreases the atomic packing density, which is also reflected in the reduction of the  $Z$  parameter.

An analysis of the structure data was also carried out using a model method [8]. Models of random atomic distribution and self-associated atomic

arrangement were used. The most probable interatomic distances  $r_1^{\text{R.D.}}$  and  $r_1^{\text{S.A.}}$  were calculated according to these models and compared with the experimental ones (Fig. 3). As it can be seen, the model of random atomic distribution is in better agreement with the experimental data. Some discrepancy between the model and the experimental values is supposed to be caused by structural inhomogeneities.

Alloys with higher Zr content (35 at.% and 45 at.%) have been studied at temperatures corresponding to mixtures of liquid tin and small

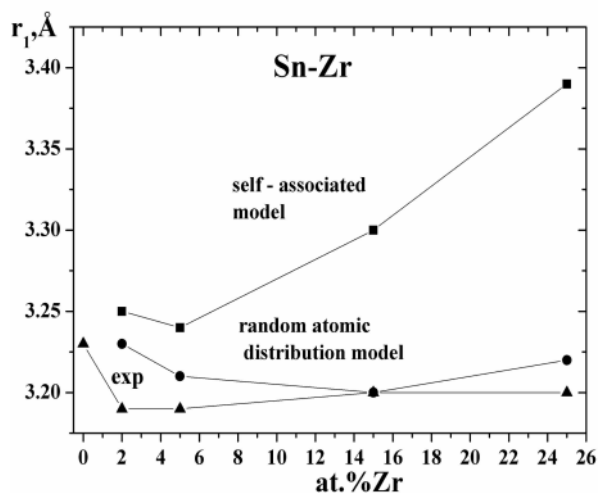


**Fig. 3** Model interpretation of structure data ( $r_1^{\text{S.A.}}$  – self-associated model;  $r_1^{\text{R.D.}}$  – random atomic distribution;  $r_1^{\text{exp.}}$  – experiment).

crystallites of a two-phase region of intermetallics formed according to a peritectic reaction (Fig. 4).

Diffraction patterns were obtained at different temperatures: 293 K, 1373 K and 1473 K. Interpretation of these curves was carried out by comparing the positions of the maxima with those of the chemical compounds  $\text{Zr}_5\text{Sn}_3$ ,  $\text{ZrSn}_2$  and Sn.

The analysis of the diffraction pattern of the sample (35 at.% Zr,  $T = 1473$  K) showed that the alloy consists of solid  $\text{Zr}_5\text{Sn}_3$  and a liquid tin-based mixture  $\text{Sn} + \text{Zr}_5\text{Sn}_3(\text{solid})$  (Fig. 4a).

Cooling to  $T = 1373$  K is accompanied by a change in the profile of the diffraction pattern. In particular, the maxima become more resolved and the asymmetry of the principal peaks transforms into separated maxima (at about  $2\theta = 32^\circ$ ). This maximum corresponds to Sn and  $\text{Zr}_5\text{Sn}_3$ . Special attention should be paid to the peak located at about  $2\theta = 35^\circ$ , which reveals significant broadening due to the appearance of  $\text{ZrSn}_2$ , whose main maxima are located just in this region. This assumption is confirmed by the appearance of a peak at  $2\theta = 41^\circ$ . These facts are the evidence that a peritectic reaction occurs according to the equilibrium phase diagram. It should also be noted that the narrower peaks observed at this temperature can be attributed to a reduction of the content of liquid Sn.

At room temperature ( $T = 293$  K) the diffraction pattern shows the existence of three phases: particularly pure solid Sn,  $\text{Zr}_5\text{Sn}_3$  and  $\text{ZrSn}_2$ .

In the case of the alloy containing 45 at.% Zr diffraction patterns were obtained for different temperatures starting from 1473 K (Fig. 4b). This temperature is somewhat above that of the peritectic reaction. The analysis of the peak positions showed that the alloy under investigation was a mixture of a

liquid Sn-rich solution and the  $\text{Zr}_5\text{Sn}_3$  chemical compound.

Upon cooling and holding at 1373 K the diffraction pattern transforms, in particular maxima arise. Peaks corresponding to the liquid phase disappear, whereas a few other peaks, corresponding to the  $\text{ZrSn}_2$  compound, appear. These facts indicate the occurrence of a peritectic reaction under these conditions. A similar behavior was observed for an alloy containing 35 at.% Zr.

At room temperature the diffraction pattern indicates the existence of the following phases:  $\text{Zr}_5\text{Sn}_3$ ,  $\text{ZrSn}_2$  and Sn. The small fraction of tin is probably caused by non equilibrium conditions for the peritectic reaction (cooling rate, concentration deviation).

We have also compared the diffraction patterns for two concentrations at room temperature. One can see some changes in the heights and widths of the peaks. These changes were attributed to the difference in the phase fractions.

From the results of the X-ray studies of liquid and solid  $\text{Sn}_{1-x}\text{Zr}_x$  alloys one can conclude that the influence of structural features in the liquid at the starting stage of the crystallization process is significant. A tendency towards the formation of chemically ordered structural units, whose structure is similar to that of intermetallics, was observed and the existence of clusters in the liquid state is possible. These clusters aggregate into larger structure units, which under equilibrium conditions of crystallization reach a critical size and become the nucleus of a solid phase. Just before the solidification process, the state of the melt, containing such clusters, is supposed to be very sensitive to external influence (pressure, uncontrolled impurities, acoustic energy, electric and magnetic fields, etc.) and cooling conditions.

In some cases the cluster aggregation process can be inhibited, resulting in overcooling. In other cases the opposite situation, where the cluster aggregation process can be stimulated, is also possible and the crystallization process will start at a higher temperature than predicted by the equilibrium phase diagram.

X-ray diffraction data registered upon slow cooling allow to determine the liquidus temperatures  $T_L$  with high accuracy (Table 1).

## Conclusions

The structure of Sn-enriched  $\text{Sn}_{1-x}\text{Ti}_x$  molten alloys shows an inhomogeneous atomic distribution at precrystallization temperatures. Zr-atoms, diluted in a matrix of tin, influence the structure of the molten alloys more significantly than can be suggested in case of a random atomic solution. An increase of the Zr-atom content is accompanied by the formation of chemically ordered microdomains. The microinhomogeneous structure formed in such a way can influence the starting process of solidification,

